

Born-Oppenheimer Breakdown in Graphene

Simone Pisana¹, Michele Lazzeri², Cinzia Casiraghi¹, Kostya S. Novoselov³,
Andre K. Geim³, Andrea C. Ferrari^{1*}, Francesco Mauri^{2†}

March 23, 2022

¹Engineering Department, Cambridge University, 9 JJ Thomson Avenue,
Cambridge CB3 0FA, UK

²IMPMC, Universités Paris 6 et 7, CNRS, IPGP, 140 rue de Lourmel, 75015
Paris, France

³Department of Physics and Astronomy, University of Manchester, Manch-
ester, M13 9PL, UK

The Born-Oppenheimer approximation (BO) [1] is the standard ansatz to describe the interaction between electrons and nuclei. BO assumes that the lighter electrons adjust adiabatically to the motion of the heavier nuclei, remaining at any time in their instantaneous ground-state. BO is well justified when the energy gap between ground and excited electronic states is larger than the energy scale of the nuclear motion. In metals, the gap is zero and phenomena beyond BO (such as phonon-mediated superconductivity or phonon-induced renormalization of the electronic properties) occur [2]. The use of BO to describe lattice motion in metals is, therefore, questionable [3, 4]. In spite of this, BO has proven effective for the accurate determination of chemical reactions [5], molecular dynamics [6, 7] and phonon frequencies [9, 8, 10] in a wide range of metallic systems. Graphene, recently discovered in the free state [11, 12], is a zero band-gap semiconductor [13], which becomes a metal if the Fermi energy is tuned applying a gate-voltage V_g [14, 12]. Graphene electrons near the Fermi energy have two-dimensional massless dispersions, described by Dirac cones. Here

*acf26@eng.cam.ac.uk

†francesco.mauri@impmc.jussieu.fr

we show that a change in V_g induces a stiffening of the Raman G peak (i.e. the zone-center E_{2g} optical phonon [15, 16]), which cannot be described within BO. Indeed, the E_{2g} vibrations cause rigid oscillations of the Dirac-cones in the reciprocal space [17]. If the electrons followed adiabatically the Dirac-cone oscillations, no change in the phonon frequency would be observed. Instead, since the electron-momentum relaxation near the Fermi level [18, 19, 20] is much slower than the phonon motion, the electrons do not follow the Dirac-cone displacements. This invalidates BO and results in the observed phonon stiffening. This spectacular failure of BO is quite significant since BO has been the fundamental paradigm to determine crystal vibrations from the early days of quantum mechanics [1, 9, 21, 8, 10].

Graphene samples are prepared by micromechanical cleavage of bulk graphite at the surface of an oxidized Si wafer with a 300 nm thick oxide layer, following the procedures described in Ref. [11]. This allows us to obtain graphene monocrystals exceeding 30 microns in size. By using photolithography, we then make Au/Cr electrical contacts, which enable the application of a gate voltage, V_g , between the Si wafer and graphene (Fig. 1A,B). The resulting devices are characterized by electric-field-effect measurements [12, 14, 22], yielding a charge carrier mobility μ of 5,000 to 10,000 cm^2/Vs at 295K and a zero-bias ($V_g=0$) doping of $\sim 10^{12} \text{ cm}^{-2}$ [23]. This is reflected in the existence of a finite gate voltage V_n at which the Hall resistance is zero and the longitudinal resistivity reaches its maximum. Accordingly, a positive (negative) $V_g - V_n$ induces an electron (hole) doping, having an excess-electron surface-concentration of $n = \eta(V_g - V_n)$. The coefficient $\eta \approx 7.2 \cdot 10^{10} \text{ cm}^{-2}/\text{V}$ is found from Hall effect measurements and agrees with the geometry of the resulting capacitor [12, 11, 14].

Unpolarized Raman spectra are measured at 295 and 200 K in ambient air and in vacuum ($< 5 \cdot 10^{-6} \text{ mbar}$), respectively, with a Renishaw spectrometer at 514nm using a $50\times$ long working distance objective, Fig. 1B. The incident power is kept well below 4mW in order to avoid sample damage or laser induced heating [15]. The Raman spectra are measured as a function of the applied V_g , Fig. 2A. Each spectrum is collected for 30 seconds. The applied gate voltage tends to move the Dirac point, especially at room temperature. We thus determine the V_g corresponding to the minimum G peak position, and use this to estimate V_n . Fig. 2A,B show that the G peak upshifts with positive applied $V_g - V_n$. It also shows a similar trend, albeit over a smaller

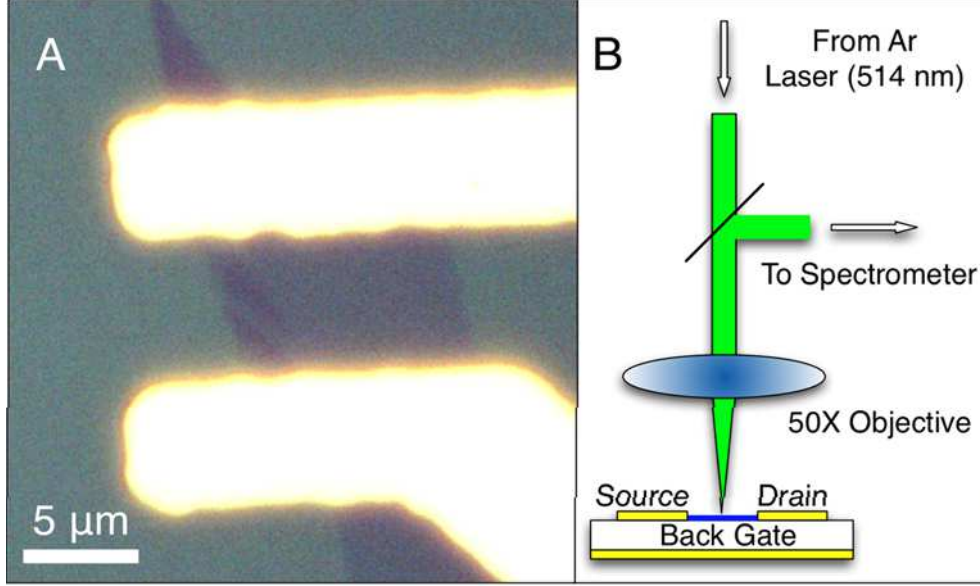


Figure 1: (A) Optical micrograph of the contacted graphene sample. (B) Schematic of the Raman+transport measurement system

voltage range, for negative V_g - V_n . This upshift for both electron and hole doping is qualitatively similar to that reported by Yan *et al.* for electrically doped graphene measured at 10K [24].

The Raman G peak of graphene corresponds to the E_{2g} phonon at Γ [15, 16]. Phonon calculations done within BO for undoped graphene and graphite, show the presence of a Kohn anomaly in the phonon dispersion of the E_{2g} mode near Γ [25]. A Kohn anomaly is the softening of a phonon of wavevector $\mathbf{q} \sim 2\mathbf{k}_F$, where \mathbf{k}_F is a Fermi surface wavevector [26]. By doping graphene, intuitively one could expect that the change in the Fermi surface should move the Kohn anomaly away from $\mathbf{q}=\mathbf{0}$ and, thus, stiffen the Γ phonon detected by Raman measurements, which would be in agreement with our experiments. To validate this picture, we need to compute the frequency of the E_{2g} mode in doped graphene.

In graphene, the electronic bands near the high-symmetry \mathbf{K} points are well described by a Dirac dispersion [13] $\epsilon(\mathbf{k}, \pi^*) = \hbar v_F k$ and $\epsilon(\mathbf{k}, \pi) = -\hbar v_F k$, where $\mathbf{k} + \mathbf{K}$ is the momentum of the Dirac Fermions, v_F is the Fermi velocity and $\hbar v_F = 5.52 \text{ eV \AA}$, from density functional theory (DFT) calculations [25] (Fig. 3A). The Dirac point is defined by the crossing of

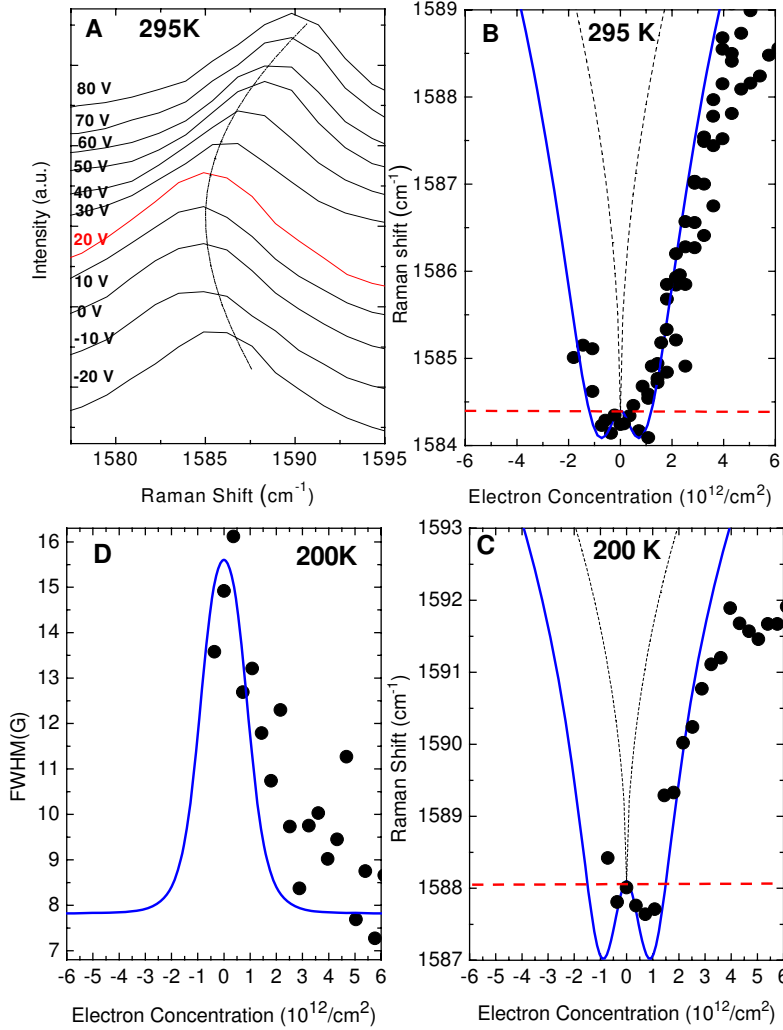


Figure 2: (A) G peak of graphene measured at room temperature as a function of V_g . The red spectrum corresponds to the Dirac point. (B-C) G peak position as a function of electron concentration at 200 and 295 K: (black dots) measurements; (red-dashed line) adiabatic Born-Oppenheimer; (blue line) finite-temperature non-adiabatic calculation from Eq. 6; (thin dashed black) simplified non-adiabatic calculation from Eq. 5. (D) G peak Full Width at Half Maximum, FWHM(G), at 200K as a function of electron concentration: (dots) measured; (Blue line) theoretical FWHM of a Voigt profile obtained from a Lorentzian component given by Eq. 7, and a constant Gaussian component of $\sim 8 \text{ cm}^{-1}$.

these conic bands and coincides with \mathbf{K} , Fig. 3A. Thus, at zero temperature, the doping-induced shift of the Fermi level from the Dirac-point is $\epsilon_F = \text{sgn}(n)\sqrt{n\pi}\hbar v_F$, where $\text{sgn}(x)$ is the sign of x .

The E_{2g} phonon in graphene consists of an in-plane displacement of the carbon atoms by a vector $\pm\mathbf{u}/\sqrt{2}$ as sketched in Fig. 3D. In presence of such atomic displacements, the bands are still described by a cone (i.e. a gap does not open) with the Dirac-point shifted from \mathbf{K} by a vector \mathbf{s} (Fig. 3B,C) [17]. In practice, the atomic-pattern of the E_{2g} vibrations is mirrored into an identical pattern of Dirac-point vibrations in the reciprocal space. The dependence of the electronic-bands on \mathbf{u} can be obtained (see supplementary information) from the DFT electron-phonon coupling matrix-elements (Eq. 6 and note 24 of Ref. [25]):

$$\epsilon(\mathbf{k}, \pi^*/\pi, \mathbf{u}) = \pm\hbar v_F |\mathbf{k} - \mathbf{s}(\mathbf{u})| \quad (1)$$

where $\mathbf{s} \cdot \mathbf{u} = 0$, $s = u\sqrt{2\langle D_{\mathbf{F}}^2 \rangle_F}/(\hbar v_F)$, and $\langle D_{\mathbf{F}}^2 \rangle_F = 45.6 \text{ (eV)}^2/\text{\AA}^{-2}$ is the deformation potential of the E_{2g} mode [27]. Eq. 1 well reproduces the modification of the DFT band structure of graphene due to a static displacement (frozen-phonon) of the atoms according to the G phonon pattern.

The knowledge of the electronic-bands (in the presence of a phonon) allows the determination of the phonon energy $\hbar\omega_{\epsilon_F}$ as a function of ϵ_F . In particular,

$$\hbar\Delta\omega = \hbar\omega_{\epsilon_F} - \hbar\omega_0 = \frac{\hbar}{2M\omega_0} \frac{d^2\Delta E}{(du)^2}, \quad (2)$$

where M is the carbon mass, $\Delta\omega \ll \omega_0$ and ΔE is the variation of the electronic energy with ϵ_F .

Within BO, $\Delta E(u)$ is computed assuming a static atomic displacement. Under this hypothesis, for any given displacement \mathbf{u} , the electrons are supposed to be in the ground state configuration, i.e. the bands $\epsilon(\mathbf{k}, \pi^*, \mathbf{u})$ are filled up to ϵ_F (Fig. 3B). Thus, the adiabatic ΔE is

$$\Delta E(u) = \frac{4A}{(2\pi^2)} \int_{\epsilon(\mathbf{k}, \pi^*, \mathbf{u}) < \epsilon_F} \epsilon(\mathbf{k}, \pi^*, \mathbf{u}) d^2k, \quad (3)$$

where we consider $\epsilon_F > 0$, $A = 5.24 \text{ \AA}^2$ is the unit-cell area, a factor 4 accounts for spin and \mathbf{K} -point degeneracy. Combining Eq. 1 and 3, we have that ΔE does not depend on \mathbf{u} and $\hbar\Delta\omega = 0$. *Thus, within BO, the Raman G peak position is independent of ϵ_F , in contrast with the trend*

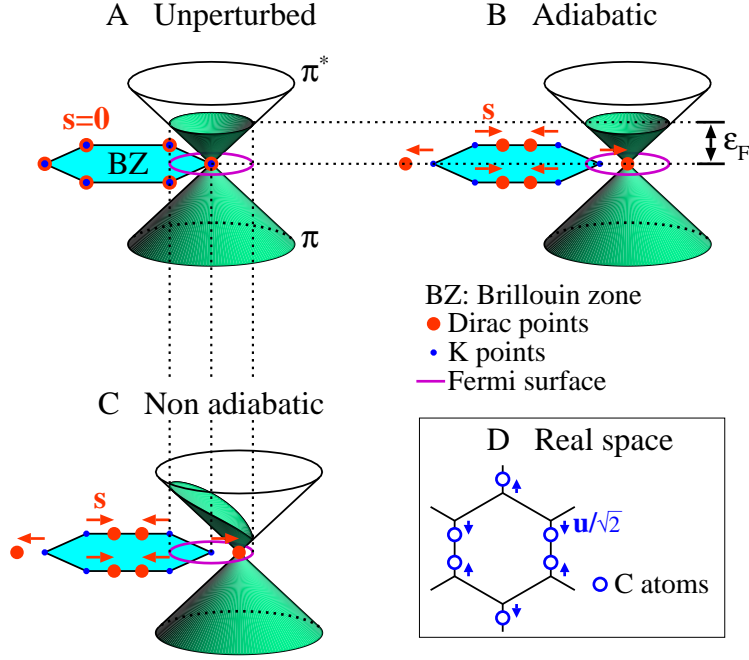


Figure 3: Schematic π band structure of doped graphene near the high symmetry \mathbf{K} point of the Brillouin zone. The filled electronic states are colored in green. (A) Bands of the perfect crystal. The Dirac point coincides with \mathbf{K} , the electronic states are filled up to the Fermi energy ϵ_F and the Fermi surface is a circle centered at \mathbf{K} . (B) Bands in presence of an E_{2g} lattice distortion. The Dirac points are displaced from \mathbf{K} by $\pm \mathbf{s}$. In the adiabatic approximation, the electrons remain in the instantaneous ground state: the bands are filled up to ϵ_F and the Fermi surface follows the Dirac-point displacement. The total electron-energy does not depend on \mathbf{s} . (C) Bands in presence of an E_{2g} lattice distortion. In the non-adiabatic case, the electrons do not have time to relax their momentum (through impurity, electron-electron and electron-phonon scattering) to follow the instantaneous ground state. In absence of scattering, the electron momentum is conserved and a state with momentum \mathbf{k} is occupied if the state with the same \mathbf{k} is occupied in the unperturbed case. As a consequence, the Fermi surface is the same as in the unperturbed case and does not follow the Dirac-cone displacement. The total electron-energy increases with s^2 resulting in the observed E_{2g} -phonon stiffening. (D) Atomic pattern of the E_{2g} lattice distortion, corresponding to the Raman G peak. The atoms are displaced from the equilibrium positions by $\pm \mathbf{u}/\sqrt{2}$. Note that the displacement pattern of the Dirac points (in reciprocal space) is identical to the displacement pattern of the carbon atoms (in real space).

reported in Fig. 2B,C. Note that Ref. [28] calculated the doping dependence of the G peak position within BO, but found significant phonon softening for increasing doping, quite the opposite of the experiments, and in contrast with our BO calculation.

The failure of the frozen-phonon calculation, urges us to re-examine the assumptions underlying BO. The E_{2g} phonon is a dynamical perturbation described by a time-dependent lattice displacement $\tilde{\mathbf{u}}(t) = \mathbf{u} \cos(\omega_0 t)$ oscillating at the G peak frequency. Within BO, it is assumed that, at any given time t , the electrons are in the adiabatic ground state of the instantaneous band structure $\epsilon(\mathbf{k}, \pi^*, \tilde{\mathbf{u}}(t))$. However, the period of the G peak vibrations is ~ 21 fs, which is much shorter than the typical electron-momentum relaxation times τ_m (due to impurity, electron-electron and electron-phonon scattering). Indeed, a τ_m of a few hundreds fs is deduced from the electron-mobility in graphene [18] and from ultra-fast spectroscopy in graphite [19, 20]. As a consequence *the electrons do not have time to relax their momenta to reach the instantaneous adiabatic ground state, as assumed in BO*. The departure from the adiabatic ground state can be accounted for in the calculation of ΔE , by filling the perturbed bands, $\epsilon(\mathbf{k}, \pi^*, \mathbf{u})$ with the occupations of the unperturbed bands $\epsilon(\mathbf{k}, \pi^*, \mathbf{0})$, as in Fig. 3C:

$$\Delta E(u) = \frac{4A}{(2\pi^2)} \int_{\epsilon(\mathbf{k}, \pi^*, \mathbf{0}) < \epsilon_F} \epsilon(\mathbf{k}, \pi^*, \mathbf{u}) d^2k + O(u^3). \quad (4)$$

This equation is valid in the limit $\epsilon_F \gg \hbar\omega_0/2$, and can be rigorously derived using time dependent perturbation theory (see supplementary information). In this case, the non-adiabatic energy, ΔE , depends on u . By replacing Eq. 1 and Eq. 4 in Eq. 2 and performing the integral we get:

$$\hbar\Delta\omega = \frac{\hbar A \langle D_{\mathbf{r}}^2 \rangle_F}{\pi M \omega_0 (\hbar v_F)^2} |\epsilon_F| = \alpha' |\epsilon_F|, \quad (5)$$

where $\alpha' = 4.39 \cdot 10^{-3}$.

The result of Eq. 5 can be extended to any ϵ_F and finite temperature T using time dependent perturbation theory [29] to obtain:

$$\hbar\Delta\omega = \alpha' P \int_{-\infty}^{\infty} \frac{[f(\epsilon - \epsilon_F) - f(\epsilon)] \epsilon^2 \text{sgn}(\epsilon)}{\epsilon^2 - (\hbar\omega_0)^2/4} d\epsilon, \quad (6)$$

where P is the principal part, and f is the Fermi-Dirac distribution at T . Fig. 2B,C shows the excellent agreement of our non-adiabatic finite T calculation (Eq. 6) with the experiments. The measured trends are also captured

by the simplified model, Eq. 5. By comparing the predictions of the BO calculation and of the non-adiabatic model, we conclude that *the stiffening of the E_{2g} mode with $|\epsilon_F|$ is due to the departure of the electron population from the adiabatic ground state.*

A pictorial interpretation of this phenomenon can be obtained by considering what happens to a filled glass when shaken horizontally. The liquid gravitational-energy and its level mimic the electronic energy ΔE and ϵ_F , respectively. The shaking frequency mimics the phonon frequency and the relaxation time of the liquid-surface mimics the electron relaxation time. If the motion of the glass is slow, the liquid surface remains flat and its gravitational-energy is independent of the glass horizontal position, as in Eq. 3 and in Fig. 3B. If the motion of the glass is rapid, the liquid surface profile is not flat and its gravitational-energy increases with the displacement of the glass, as in Eq. 4 and Fig. 3C. To push the analogy even further, one should use a non-cylindrical glass, for which the liquid surface increases with the liquid level. In this case, the higher the liquid-level, the larger the difference between the gravitational energies in the fast- and slow-shaken glass. Indeed, in graphene, the higher the Fermi level, the larger the difference between the non-adiabatic ΔE and the adiabatic ΔE . This causes the observed stiffening of the phonon frequency with ϵ_F .

The validity of our model is further confirmed by the analysis of the G peak linewidth. The phonon decaying into an electron-hole pair gives the most important contribution to the homogeneous broadening of the E_{2g} phonon. The full-width at half-maximum, γ , can be computed extending to finite T and $\epsilon_F \neq 0$ the results of Ref. [27]:

$$\gamma = \frac{\pi^2 \omega_0 \alpha'}{c} \left[f \left(-\frac{\hbar \omega_0}{2} - \epsilon_F \right) - f \left(\frac{\hbar \omega_0}{2} - \epsilon_F \right) \right], \quad (7)$$

where c is the speed of light. At $T = 0$, $\gamma = 11 \text{ cm}^{-1}$ for $\epsilon_F = 0$ and γ drops to zero for $\epsilon_F > \hbar \omega_0/2$ because the scattering process is forbidden by the Pauli exclusion principle [27]. Fig. 2D shows a good agreement between the experimental and theoretical γ , once a constant inhomogeneous Gaussian broadening of $\sim 8 \text{ cm}^{-1}$ is added to the electron-phonon contribution of Eq. 7.

Concluding, the observed stiffening of the E_{2g} phonon in doped graphene represent a spectacular failure of the adiabatic Born-Oppenheimer approximation. Within BO, the energy of a zone-center phonon is determined by two contributions: the distortion of the electronic bands, associated with the

phonon displacement, and the consequent rearrangement of the Fermi surface. These two contributions cancel out exactly in graphene because of the peculiar rigid motion of the Dirac-cones, associated to the E_{2g} phonon. In general, a correct phonon treatment *should not* include the BO Fermi-surface rearrangement, whenever the electron-momentum relaxation time (near ϵ_F) is longer than the phonon period. We anticipate the failure of BO, shown here, to have important consequences in the description of vibrational properties of carbon-nanotubes and in phonon-mediated superconductors.

Acknowledgments The authors thank P. Kim and A. Pinczuk for useful discussions and for sending a preprint of Ref. [24]. A. C. F. acknowledges funding from the Royal Society and The Leverhulme Trust. Calculations were performed at the IDRIS supercomputing center.

References

- [1] M. Born, J. R. Oppenheimer. Zur Quantentheorie der Molekeln. Ann. Phys. **84**, 457 (1927).
- [2] G. Grimvall. The electron-phonon interaction in metals. North-Holland, Amsterdam (1981).
- [3] Y. S. Ponosov, G. A. Bolotin, C. Thomsen, M. Cardona. Raman scattering in Os: nonadiabatic renormalization of the optical phonon self energies. Phys. Stat. Sol. B **208**, 257 (1988).
- [4] J. D. White, J. Chen, D. Matsiev, D. J. Auerbach, A. M. Wodtke. Conversion of large-amplitude vibration to electron excitation at a metal surface. Nature **433**, 503 (2005).
- [5] G. J. Kroes, A. Gross, E. J. Baerends, M. Scheffler, D. A. McCormack. Quantum theory of dissociative chemisorption on metal surfaces. Acc. Chem. Res. **35**, 193 (2002).
- [6] Alfe D., Gillan M.J., Price G.D., The melting curve of iron at the pressures of the Earth's core from ab initio calculations. Nature **401** 462 (1999).

- [7] B.G. Walker, C. Molteni, N. Marzari. Ab initio molecular dynamics of metal surfaces. *J. Phys.: Condens. Matter* **16**, S2575 (2004).
- [8] S. Baroni, S. De Gironcoli, A. Dal Corso, P. Giannozzi. Phonons and related crystal properties from density functional perturbation theory. *Rev. Mod. Phys.* **73**, 515 (2001).
- [9] G. V. Chester. The theory of interaction of electrons with lattice vibrations in metals. *Adv. Phys* **10**, 357 (1961).
- [10] S. Y. Savrasov, D. Y. Savrasov. Electron-phonon interactions and related physical properties of metals from linear-response theory. *Phys. Rev. B* **54**, 16487 (1996).
- [11] K.S. Novoselov, D. Jiang, F. Schedin, T.J. Booth, V.V. Khotkevich, S.M. Morozov, and A.K. Geim. Two dimensional atomic crystals. *Proc. Natl Acad. Sci. USA* **102**, 10451-10453 (2005).
- [12] K.S. Novoselov, A.K. Geim, S.V. Morozov, D. Jiang, Y. Zhang, S.V. Dubonos, I.V. Grigorieva, and A.A. Firsov. Electric field effect in atomically thin carbon films, *Science* **306**, 666-669 (2004).
- [13] P. R. Wallace. The Band theory of graphite. *Phys. Rev.* **71**, 622 (1947).
- [14] K.S. Novoselov, A.K. Geim, S.M. Morozov, M.I. Katsnelson, I.V. Grigorieva, S.V. Dubonos, and A.A. Firsov. Two dimensional gas of massless Dirac fermions in graphene. *Nature* **438**, 197-200 (2005).
- [15] A. C. Ferrari, J. C. Meyer, V. Scardaci, C. Casirgahi, M. Lazzeri, F. Mauri, S. Piscanec, D. Jiang, K. S. Novoselov, S. Roth, A. K. Geim. Raman spectrum of graphene and graphene layers. *Phys. Rev. Lett.* **97**, 187401 (2006).
- [16] F. Tuinstra, J. Koenig. Raman spectrum of graphite *J. Chem. Phys.* **53**, 1126 (1970).
- [17] O. Dubay and G. Kresse. Accurate density functional calculations for the phonon dispersion relations of graphite layer and carbon nanotubes. *Phys. Rev. B* **67**, 035401 (2003).

- [18] Zhang Y., Jiang Z., Small J. P., Purewal M. S., Tan Y.-W., Fazlollahi M., Chudow J. D., Jaszczak J. A., Stormer H. L., and Kim P. Landau-Level Splitting in Graphene in High Magnetic Fields. *Phys. Rev. Lett.* **96**, 136806 (2006).
- [19] G. Moos, C. Gahl, R. Fasel, M. Wolf, T. Hertel. Anisotropy of quasi-particle lifetimes and the role of disorder in graphite from ultrafast time-resolved photoemission spectroscopy. *Phys. Rev. Lett.* **87**, 267402 (2001).
- [20] T. Kampfrath, L. Perfetti, F. Schapper, C. Frischkorn, M. Wolf. Strongly coupled optical phonons in the ultrafast dynamics of electronic energy and current relaxation in graphite. *Phys. Rev. Lett.* **95**, 187403 (2005).
- [21] R. M. Pick, M. H. Cohen, R. M. Martin. Microscopic theory of force constants in the adiabatic approximation. *Phys. Rev.* **1** 910, (1970).
- [22] Y. Zhang, Y. W. Tan, H. L. stormer, P. Kim. Experimental observation of the quantum Hall effect and Berry's phase in graphene. *Nature* **438**, 201 (2005).
- [23] F. Schedin, K. S. Novoselov, S. V. Morozov, D. Jiang, E. H. Hill, P. Blake, A. K. Geim. Detection of individual gas molecules by graphene sensors. *Cond. Mat.* 0610809.
- [24] J. Yan, Y. Zhang, P. Kim, A. Pinczuk, unpublished
- [25] S. Piscanec, M. Lazzeri, F. Mauri, A.C. Ferrari, and J. Robertson. Kohn anomalies and electron phonon interactions in graphite. *Phys. Rev. Lett.* **93**, 185503 (2004).
- [26] W. Kohn. Image of the Fermi Surface in the Vibration Spectrum of a Metal. *Phys Rev. Lett.* **2**, 393 (1959).
- [27] M. Lazzeri, S. Piscanec, F. Mauri, A.C. Ferrari, and J. Robertson. Phonon linewidths and electron-phonon coupling in graphite and nanotubes. *Phys. Rev. B* **73**, 155426 (2006).
- [28] A. H. Castro Neto, F. Guinea. Electron Phonon coupling and Raman spectroscopy in disordered graphene, cond-mat/0608343.v3 (2006).

- [29] M. Lazzeri, F. Mauri, Non-adiabatic Kohn-anomaly in a doped graphene monolayer, cond-mat/0611708 (2006).

Supplementary Information

Derivation of Eq. 1

The electronic Hamiltonian for the π, π^* basis can be written as a 2×2 matrix:

$$H(\mathbf{k}, \mathbf{0}) = \begin{pmatrix} \hbar v_F k & 0 \\ 0 & -\hbar v_F k \end{pmatrix}, \quad (8)$$

where \mathbf{k} is a small in plane wave-vector and $\mathbf{K} + \mathbf{k}$ is the electronic momentum. Let us consider a distortion of the lattice according to a $\Gamma - E_{2g}$ phonon pattern (note that the $\Gamma - E_{2g}$ phonon is doubly degenerate). At the lowest order the π -bands Hamiltonian changes as

$$H(\mathbf{k}, \mathbf{u}) = H(\mathbf{k}, \mathbf{0}) + \frac{\partial H(\mathbf{k}, \mathbf{0})}{\partial u} u \quad (9)$$

where u is the phonon normal coordinate (the two atoms in the unit-cell are displaced by $\pm u/\sqrt{2}$ along a given direction in the plane). $\partial H/(\partial u)$ can be obtained from the ab-initio deformation potential matrix elements. Following Ref. [25] (Eq.6 and note 24) and Ref. [27], for the E_{2g} phonon mode and for a small \mathbf{k}

$$\left| \langle \mathbf{k}\pi^* | \frac{\partial H}{\partial u} | \mathbf{k}\pi^* \rangle \right|^2 = \left| \langle \mathbf{k}\pi | \frac{\partial H}{\partial u} | \mathbf{k}\pi \rangle \right|^2 = \langle D_{\Gamma}^2 \rangle_F [1 + \cos(2\theta)] \quad (10)$$

$$\left| \langle \mathbf{k}\pi^* | \frac{\partial H}{\partial u} | \mathbf{k}\pi \rangle \right|^2 = \langle D_{\Gamma}^2 \rangle_F [1 - \cos(2\theta)], \quad (11)$$

where $|\mathbf{k}\pi/\pi^*\rangle$ are the electronic states with momentum $\mathbf{K} + \mathbf{k}$ and θ is the angle between \mathbf{k} and the direction perpendicular to the atomic vibration. Taking the square root of Eqs. 10, 11 and inserting them into Eq. 9

$$H(\mathbf{k}, \mathbf{u}) = \begin{pmatrix} \hbar v_F k & 0 \\ 0 & -\hbar v_F k \end{pmatrix} + \sqrt{2\langle D_{\Gamma}^2 \rangle_F} \begin{pmatrix} \cos(\theta) & \sin(\theta) \\ \sin(\theta) & -\cos(\theta) \end{pmatrix} u. \quad (12)$$

The eigenvalues of Eq. 12 are then

$$\epsilon = \pm \hbar v_F \sqrt{k^2 + s^2 + 2ks \cos(\theta)} = \pm \hbar v_F |\mathbf{k} - \mathbf{s}(\mathbf{u})|, \quad (13)$$

where \mathbf{s} is defined in the main text.

Derivation of Eq. 4

Considering the Taylor expansion of $\Delta E(u)$ in u , Eq. 4 is equivalent to:

$$\frac{d^2}{(du)^2} \Delta E(u) = \frac{d^2}{(du)^2} \left\{ \frac{4A}{(2\pi)^2} \int_{\epsilon(\mathbf{k}, \pi^*, \mathbf{0}) < \epsilon_F} \epsilon(\mathbf{k}, \pi^*, \mathbf{u}) d^2k \right\}. \quad (14)$$

In this section, we will demonstrate that

$$\hbar \Delta \omega = \frac{\hbar}{2M\omega_0} \frac{d^2}{(du)^2} \left\{ \frac{4A}{(2\pi)^2} \int_{\epsilon(\mathbf{k}, \pi^*, \mathbf{0}) < \epsilon_F} \epsilon(\mathbf{k}, \pi^*, \mathbf{u}) d^2k \right\}, \quad (15)$$

at $T = 0$ and under the condition

$$\epsilon_F \gg \hbar \omega_0 / 2. \quad (16)$$

Using Eq. 2, Eq. 4 will then immediately follow.

Within time dependent perturbation theory, $\hbar \Delta \omega$ is (see Eq. 10 of Ref. [29]):

$$\hbar \Delta \omega = \frac{\hbar}{2M\omega_0} [F_0^{\epsilon_F}(\omega_0) - F_0^0(\omega_0)]. \quad (17)$$

were at $T = 0$,

$$F_0^{\epsilon_F}(\omega_0) = \frac{2}{N_{\mathbf{k}}} \sum_{\mathbf{k}, o, e} |D_{\mathbf{k}o, \mathbf{k}e}|^2 \left\{ \frac{1}{\epsilon_{\mathbf{k}o} - \epsilon_{\mathbf{k}e} + \hbar \omega_0} + \frac{1}{\epsilon_{\mathbf{k}o} - \epsilon_{\mathbf{k}e} - \hbar \omega_0} \right\}. \quad (18)$$

Here the index o and e denotes the occupied ($\epsilon_{\mathbf{k}o} < \epsilon_F$) and empty bands ($\epsilon_{\mathbf{k}e} > \epsilon_F$), and

$$D_{\mathbf{k}o, \mathbf{k}e} = \langle \mathbf{k}o | \frac{\partial H}{\partial u} | \mathbf{k}e \rangle. \quad (19)$$

Now we consider only the π and π^* bands and we substitute $1/N_{\mathbf{k}} \sum_{\mathbf{k}}$ with $A/(2\pi)^2 \int d^2k$, where A is the unit-cell area and the integral is restricted on a circle of radius \bar{k} , centered on \mathbf{K} . Assuming a Dirac dispersion for the π and π^* bands, $\epsilon_{\mathbf{k}e} - \epsilon_{\mathbf{k}o} \geq 2\epsilon_F$. Thus, if the condition of Eq. 16 holds, $|\epsilon_{\mathbf{k}e} - \epsilon_{\mathbf{k}o}| \gg \hbar \omega_0$ and the $\hbar \omega_0$ in the denominators of Eq. 18 can be neglected. Eq. 18 becomes

$$F_0^{\epsilon_F} = \frac{8A}{(2\pi)^2} \int_{\epsilon(\mathbf{k}, \pi^*, \mathbf{0}) > \epsilon_F, k < \bar{k}} \frac{|D_{\mathbf{k}\pi^*, \mathbf{k}\pi}|^2}{\epsilon(\mathbf{k}, \pi, \mathbf{0}) - \epsilon(\mathbf{k}, \pi^*, \mathbf{0})} d^2k, \quad (20)$$

where $\epsilon(\mathbf{k}, \pi/\pi^*, \mathbf{0})$ are the bands of the undistorted graphene structure. From Eq. 17,

$$\hbar\Delta\omega = \frac{\hbar}{2M\omega_0} \left\{ -\frac{8A}{(2\pi)^2} \int_{\epsilon(\mathbf{k}, \pi^*, \mathbf{0}) < \epsilon_F} \frac{|D_{\mathbf{k}\pi^*, \mathbf{k}\pi}|^2}{\epsilon(\mathbf{k}, \pi, \mathbf{0}) - \epsilon(\mathbf{k}, \pi^*, \mathbf{0})} d^2k \right\}. \quad (21)$$

From textbook static second order perturbation theory

$$\frac{1}{2} \frac{d^2\epsilon(\mathbf{k}, \pi^*, \mathbf{u})}{(du)^2} \Big|_{u=0} = \frac{|D_{\mathbf{k}\pi^*, \mathbf{k}\pi}|^2}{\epsilon(\mathbf{k}, \pi^*, \mathbf{0}) - \epsilon(\mathbf{k}, \pi, \mathbf{0})}. \quad (22)$$

Substituting Eq. 22 in Eq. 21 we have

$$\hbar\Delta\omega = \frac{\hbar}{2M\omega_0} \left\{ \frac{4A}{(2\pi)^2} \int_{\epsilon(\mathbf{k}, \pi^*, \mathbf{0}) < \epsilon_F} \frac{d^2\epsilon(\mathbf{k}, \pi^*, \mathbf{u})}{(du)^2} d^2k \right\}. \quad (23)$$

Eq. 15 is, finally, obtained by taking the derivation with respect to u in Eq. 23 outside the integral.